Comparison of surface-potential-based and charge-based MOSFET core models

Authors: C. Galup-Montoro (1), M. Schneider (1), V. C. Pahim (1), and R. Rios (2)
(1) Federal University of Santa Catarina,
(2) Intel Corporation

ABSTRACT

Since the next generation MOSFET model will be based on either surface potential or inversion charge, a comparison between the two approaches is timely. In this paper, we will analyze in some detail the fundamentals of the two approaches. We will compare the expressions for inversion charge and gate capacitance.

1 INTRODUCTION

The modeling of MOS transistors for integrated circuit design has been driven by the needs of digital circuit simulation for many years. The present trend toward mixed analog-digital chips creates a necessity for MOSFET models appropriate for analog and RF design as well [1, 2, 3, 4].

Strong inversion used to be the prevailing MOS operation region, but as a consequence of the technological trend toward shorter channel lengths and reduced supply voltages, MOS devices now often operate in the moderate and weak inversion regions [5].

Conventional models, such as BSIM [6], are direct models since the drain current and the terminal charges are explicit functions of the terminal voltages. Since these direct models use mathematical smoothing functions to describe the transition between weak and strong inversion, they are not accurate enough to represent the moderate inversion region, widely employed in low supply voltage circuits [3, 4].

Currently, there are essentially two alternative approaches to direct models, namely surface-potential-based (ϕ_s-based) [1, 3, 4] and inversion-charge-based (q_i-based) [2, 7, 8, 9, 10] models. In these two indirect models, the drain current and the terminal charges are indirect functions of the terminal voltages through either the surface potential or the inversion charge density. One of these two approaches will probably form the basis for the next generation MOSFET model.

The accurate calculation of the surface potential [4, 19], once a big issue, is no longer a problem; in fact, the surface potential can be calculated within machine tolerances and with no significant burden in relation to the overall compact model calculations. Conventional surface potential models based on the original charge-sheet approximation of Brews [13] do not lead to a practical result due to difficulties in introducing velocity saturation effects for short-channels and obtaining closed-form self-consistent charges for the device terminals. Practical compact ϕ_s-based models (MM11, SP) use linearization of the surface potential vs. inversion charge density in a similar way as q_i-based models do [3, 4].

In regard to q_i-based models, the inversion charge density is approximated using the unified charge control model (UCCM) [8].

Briefly, ϕ_s-based and q_i-based models have a common background, but enough differences between them exist to motivate model developers to support either approach. Because the complete transistor model, including the different physical effects relevant to advanced technologies, is very complex, we will reduce our comparison to the core models based on either surface potential or inversion charge.

For a classical (as opposed to quantum mechanical) long-channel MOSFET, considering constant mobility, the main characteristics of the transistor, drain current, total charges, transconductances, and capacitive coefficients can be calculated in terms of the inversion and bulk charge densities. Consequently, we will limit this paper to a comparison of the inversion charge and gate capacitance obtained from either ϕ_s-based or q_i-based models.

2 ACCURATE LONG-CHANNEL MODEL

For a long-channel device, the *gradual channel approximation* [3, 11] is valid, i.e., the longitudinal (x-direction) component of the electrical field can be assumed to be much smaller than the transversal (y-direction) component.

A) General analysis for charge and potential

The electron and hole densities, n and p, are given by Maxwell-Boltzmann statistics. In the gradual channel approximation, the Poisson equation can be written [3, 11] as:

$$\frac{d^2\phi}{dy^2} = \frac{qN_A}{\varepsilon_s}\left(1 - e^{-\phi/\phi_t} + e^{(\phi - V_C - 2\phi_F)/\phi_t}\right) \quad (1)$$

where ϕ is the eletrostatic potential, ϕ_t is the thermal voltage, V_C is the channel-to-bulk voltage, ϕ_F is the bulk Fermi potential, N_A is the doping concentration, q is the electron charge and ε_s is the permittivity of silicon.

The total charge Q_C' per unit area in the semiconductor can be obtained from Gauss' law:

$$Q_C' = \varepsilon_s \frac{d\phi}{dy}\Big|_{y=0} \quad (2)$$

Applying Gauss' theorem at the oxide interface, Q_C' can also be related to the applied gate bias:

$$Q_C' = -C_{ox}'\left(V_G - V_{FB} - \phi_s\right) \quad (3a)$$

where C'_{ox} is the oxide capacitance per unit area and V_{FB} is the flat band voltage.

Since $Q'_C = -Q'_G$ by charge conservation, the gate electrode charge per unit area is given by:

$$Q_G' = C_{ox}'\left(V_G - V_{FB} - \phi_s\right) \quad (3b)$$

Using (1-3), an implicit relation for the surface potential is found [3, 11]

$$\left(V_G - V_{FB} - \phi_s\right)^2 = \gamma^2 \phi_t e^{-(2\phi_F + V_C)/\phi_t}\left(e^{\phi_s/\phi_t} - 1\right) + \gamma^2\left(\phi_s + \phi_t\left(e^{-\phi_s/\phi_t} - 1\right)\right) \quad (4a)$$

where γ is the body factor.

If $\phi_S > 6\phi_t$, we can approximate (4a) by

$$\left(V_G - V_{FB} - \phi_s\right)^2 = \gamma^2\left(\phi_t e^{(\phi_s - 2\phi_F - V_C)/\phi_t} + \phi_s - \phi_t\right) \quad (4b)$$

B) I-V characteristic

For the calculation of the current I_{DS} that flows from drain to source, it is assumed that the hole current as well as recombination/generation can be neglected [3,11]. In the ideal case, it is furthermore assumed that there is a current flow in the *x*-direction only. In other words, the bulk current I_B and gate current I_G are zero [11]. Assuming the mobility μ to be independent of bias and position, the channel current can be written [11, 12] as

$$I_{DS} = -\mu W Q_I' \frac{dV_C}{dx} \quad (5)$$

Integrating (5) along the channel, from source to drain, [11, 12] yields:

$$I_{DS} = -\frac{\mu W}{L}\int_{V_S}^{V_D} Q_I' dV_C \quad (6)$$

The very general equation (6) clearly indicates the relevance of the inversion charge density for MOSFET modeling.

Finally, the double integral equation for I_{DS} commonly referred to as the Pao-Sah model is obtained using the accurate expression (7) [11] for Q_I' in (6),

$$Q_I' = -qN_A e^{-(2\phi_F + V_C)/\phi_t}\int_0^{\phi_s} \frac{e^{\phi/\phi_t}}{\xi(\phi)} d\phi \quad (7)$$

with $\xi(\phi) = -\frac{d\phi}{dy}$.

3 BASIC APPROXIMATIONS FOR COMPACT MODELS

A) Charge-sheet approximation

The *charge-sheet approximation* ignores the potential drop across the inversion layer, for the calculation of the bulk charge density Q_B'. According to the charge-sheet approximation, Q_B' is given by

$$Q_B' = -sign(\phi_s) C_{ox}' \gamma \sqrt{\phi_s + \phi_t\left(e^{-\phi_s/\phi_t} - 1\right)} \quad (8)$$

Expression (8) gives a continuous model from accumulation through depletion to inversion. From (3a) and (8) and invoking charge conservation, the inversion charge density Q_I' is expressed as

$$Q_I' = -C_{ox}'\left(V_G - V_{FB} - \phi_s + \frac{Q_B'}{C_{ox}'}\right) \quad (9)$$

For ϕ_s-based models, one can calculate ϕ_s iteratively using (4a) [4,19] and the resultant value is used to calculate Q_G', Q_B' and Q_I' from (3b), (8) and (9), respectively.

The charge sheet current expression results from an additional hypothesis as explained below.

Differentiating (4b) with respect to ϕ_s we get [14, 21]

$$\frac{dV_C}{d\phi_s} = 1 + \frac{C_{ox}' + C_b'}{C_i'} \quad (10)$$

This result can be easily interpreted using Fig. 1 [15], a description of the three-terminal MOS structure as a capacitive model based on the general expression (4b). Note that expression (10) is more general than the charge-sheet approximation because it has been derived [14] from the general equation (4b) without any further approximations.

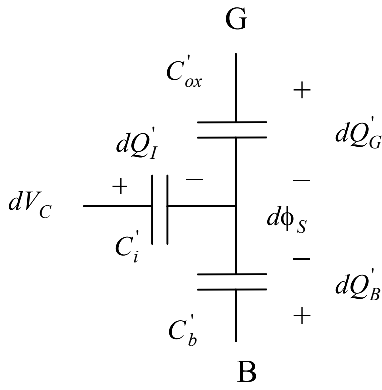

Fig. 1: Small-signal model for the three terminal MOSFET

Because the second term in the right-hand side of (10) is relevant for small Q'_I only (weak inversion), we can approximate the inversion capacitance in (10) [14, 21] by

$$C'_i = -\frac{Q'_I}{\phi_t} \tag{11}$$

Calculating C'_b in terms of Q'_I from expression (9) for constant V_G yields

$$C'_b = -\frac{dQ'_B}{d\phi_s} = \frac{dQ'_I}{d\phi_s} - C'_{ox} \tag{12}$$

Substituting (11) and (12) into (10) we get [20, 21]

$$\frac{dV_C}{d\phi_s} = 1 - \frac{\phi_t}{Q'_I}\frac{dQ'_I}{d\phi_s} \tag{13}$$

Finally, from (5) and (13) *the charge sheet current expression* results.

$$I_{DS} = I_{drift} + I_{diff} = -\mu W Q'_I \frac{d\phi_S}{dx} + \mu W \phi_t \frac{dQ'_I}{dx} \tag{14}$$

B) Linearized q_i-based models

In this section we will present a new improved version of the linearized q_i-based model. Compared to the equations published in [15], we have included here an additional term (ϕ_t), which corresponds to the hole contribution, into the bulk charge. As will be shown in the simulation section, this small term has significant impact on the model accuracy.

In inversion, (9) reduces [11] to

$$Q'_I = -C'_{ox}\left(V_G - V_{FB} - \phi_s - \gamma\sqrt{\phi_s - \phi_t}\right) \tag{15}$$

since the exponential term in (8) becomes negligible.

Expanding (15) in power series about ϕ_{Sa} (value of surface potential deep in weak inversion, neglecting channel charge) we obtain, for constant V_G [2,14]:

$$Q'_I \cong C'_{ox} n\left[\phi_s - \phi_{sa}\right] \tag{16a}$$

$$dQ'_I \cong nC'_{ox} d\phi_S \tag{16b}$$

$$n = 1 + \frac{C'_b}{C'_{ox}} = 1 + \frac{\gamma}{2\sqrt{\phi_{Sa} - \phi_t}} \tag{16c}$$

$$\sqrt{\phi_{Sa} - \phi_t} = \sqrt{V_G - V_{FB} - \phi_t + \frac{\gamma^2}{4}} - \frac{\gamma}{2} \tag{16d}$$

C'_b is the depletion capacitance calculated assuming the inversion charge to be negligible and n is the slope factor, slightly dependent on the gate voltage.

The channel charge density for which the diffusion current equals the drift current will be designated the **pinch-off charge density** Q'_{IP}. The value of Q'_{IP} is readily derived from the substitution of (16b) into (14), resulting [2,16] in

$$Q'_{IP} = -nC'_{ox}\phi_t \tag{17}$$

The channel-to-substrate voltage (V_C) for which the channel charge density equals Q'_{IP} is called the **pinch-off voltage** V_P.

Using approximation (16a) to calculate the surface potential ϕ_{SP} at pinch-off gives

$$\phi_{SP} = \phi_{Sa} - \phi_t \tag{18}$$

In order to calculate the pinch-off voltage, we can use (19), following from (4b) and (15):

$$Q'_I = -\gamma C'_{ox}\left[\sqrt{\phi_S + \phi_t e^{(\phi_S - 2\phi_F - V_C)/\phi_t} - \phi_t} - \sqrt{\phi_S - \phi_t}\right] \tag{19}$$

Substituting ϕ_S, V_C, and Q'_I with ϕ_{SP}, V_P, and Q'_{IP}, respectively, in (19) and linearizing (19) around ϕ_{SP}, results in

$$V_P = \phi_{Sa} - 2\phi_F - \phi_t\left(1 + \ln\left(\frac{n}{n-1}\right)\right) \tag{20}$$

4 UNIFIED CHARGE CONTROL MODEL

Even though the UCCM has been presented as a semi-empirical model, we have shown in [15] that the UCCM (21) can be readily derived using two approximations:

1. the depletion capacitance per unit area is assumed to be constant along the channel and is calculated assuming the inversion charge to be negligible in the potential balance equation;
2. the inversion capacitance is proportional to the inversion charge density, a hypothesis already included in the expression of the charge-sheet current.

The resultant UCCM is given by

$$V_P - V_C = \phi_t\left[\frac{Q'_{IP} - Q'_I}{nC'_{ox}\phi_t} + \ln\left(\frac{Q'_I}{Q'_{IP}}\right)\right] \tag{21}$$

A fundamental property of (21) is that, in weak inversion, it is asymptotically coincident with the charge-sheet model. Substituting (17) and (20) into (21) and considering $Q'_I \rightarrow 0$, it follows that

$$Q'_I = -\frac{\sqrt{2q\varepsilon_S N_A}}{2\sqrt{\phi_{sa} - \phi_t}}\phi_t e^{(\phi_{sa} - 2\phi_F)/\phi_t} e^{-V_C/\phi_t} \tag{22}$$

We will call this improved version of the UCCM, which includes the additional term ϕ_t into the bulk charge, as UCCM$^+$.

Expression (22) is also the asymptotic expression in weak inversion for the calculation of the inversion charge using equations (4a), (8) and (9).

Substituting the first order approximation of V_P presented in [5]

$$V_P \cong \frac{V_G - V_{T0}}{n} \tag{23}$$

into (21) gives

$$Q'_{IP} - Q'_I + nC'_{ox}\phi_t \ln\left(\frac{Q'_I}{Q'_{IP}}\right) = C'_{ox}\left(V_G - V_{T0} - nV_C\right) \tag{24}$$

Equation (24) is useful for hand analysis, but the exponential dependence of Q'_I on V_P in weak inversion precludes (24) or expressions based on approximations of the pinch-off voltage from being used for accurate modeling.

As a final comment about the unicity of the UCCM, let us consider the linear relationship between inversion charge and surface potential, and the consistency between the expressions of the drain current using either the drift/diffusion equation (14) or the quasi-Fermi potential formulation (5):

$$I_D = \frac{\mu W}{nC'_{ox}}\left(-Q'_I + nC'_{ox}\phi_t\right)\frac{dQ'_I}{dx} = -\mu W Q'_I \frac{dV_C}{dx} \tag{25}$$

From (25) it follows that

$$dQ'_I\left(\frac{1}{nC'_{ox}} - \frac{\phi_t}{Q'_I}\right) = dV_C \tag{26}$$

Equation (26) represents the UCCM in differential form.

5 COMPARISON BETWEEN INVERSION CHARGE DENSITY MODELS

The full numerical solution of the Poisson equation (1) will be used as a baseline for comparison of charges. Expression (1) is solved by finite differences with a non-uniform discrete mesh in y.

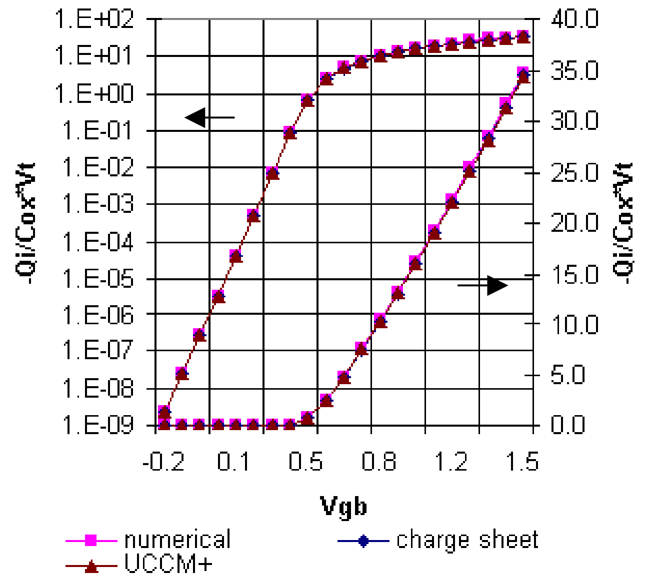

Fig. 2: Inversion charge density

For the simulations, the following parameters were used (unless specified otherwise): temperature=27 °C, oxide thickness= 2nm, doping concentration= 2E18 cm^{-3}.

As shown in Fig.2, UCCM^{+} and the ϕ_s-based model give very good approximations for the inversion charge densities from weak, through moderate to strong inversion.

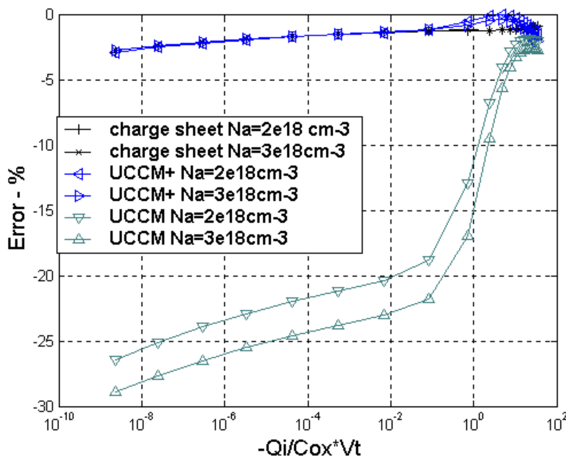

Fig. 3: Error in inversion charge density for two doping concentrations

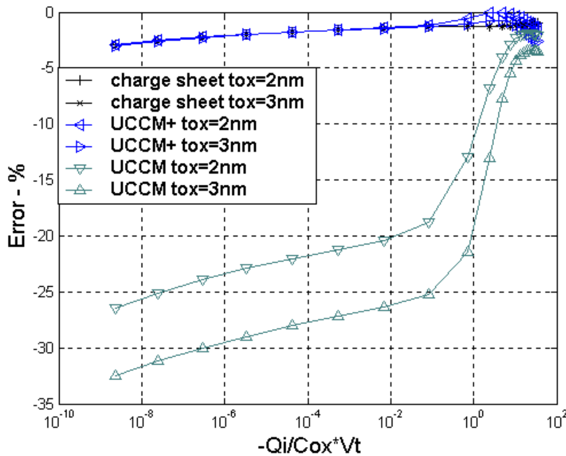

Fig. 4: Error in inversion charge density for two oxide thicknesses

As shown in Fig. 3 and Fig.4, the old version of UCCM is not accurate in WI. Moreover, the amount of error for the original UCCM strongly depends on the physical parameters Tox and Na as well as on operating temperature, which undermines the predictive qualities of the model. This is also the case for other proposed variants of the qi-based approach. Concerning the ϕ_s-based charge-sheet model and UCCM^{+}, both approaches give errors less than 3% under normal bias conditions and for a wide range of physical parameters. UCCM^{+} and charge sheet are strictly equivalent in weak inversion as expected. An interesting result from Figs. 3 and 4 is that UCCM^{+} gives a better approximation than the charge-sheet model for moderate inversion while in strong inversion the opposite is observed. The better accuracy of the UCCM^{+} in moderate inversion is related to the fact that the capacitive model on which the UCCM^{+} is based is more general than the charge-sheet approximation. In strong inversion the value of the inversion capacitance $(-Q_I^{'}/\phi_t)$ used in UCCM^{+} is less accurate and the charge-sheet model gives a better result.

6 COMPARISON BETWEEN CAPACITIVE MODELS

All charges are obtained naturally in the ϕ_s-based model, but there is a need for supplementary bulk and/or gate charge models in q_i-based approaches.

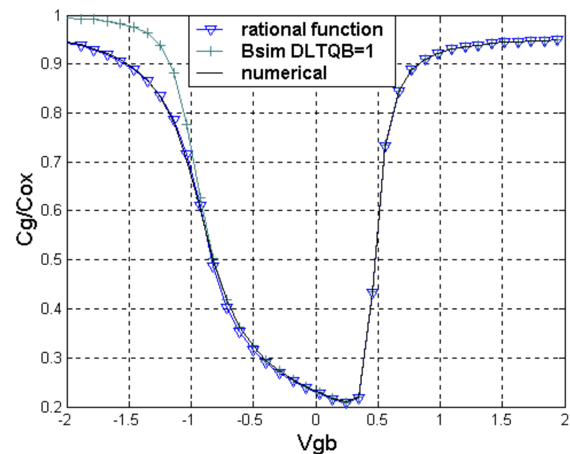

Fig.5: Gate capacitance

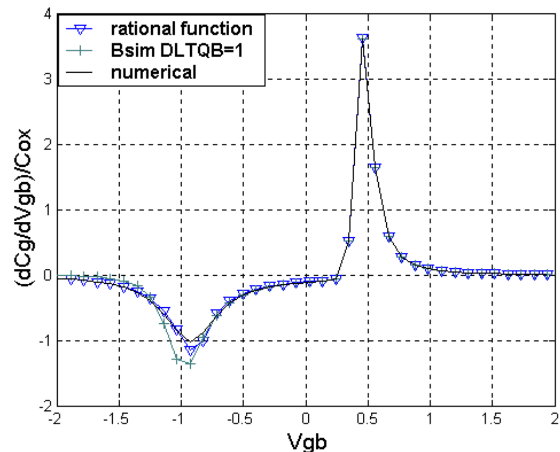

Fig.6: Derivative of gate capacitance

Figure 5 compares two approximate models of the gate capacitance from [17] and [18] against the ϕ_s-based model .

The BSIM5 curve [17] is the result of an empirical model, which is not accurate in accumulation. The model we have used for the bulk capacitance in Fig. 5 approximates it in accumulation by a rational function that gives the correct asymptotic behavior in accumulation and ensures continuity for the first (Fig. 6) and second derivatives of the capacitance. The drawback of the model based on this rational function is the cumbersome expression for the bulk charge.

7 CONCLUSIONS

The main approximations behind the surface-potential-based and the charge-based models were analyzed. A new high accuracy charge model ($UCCM^+$) was achieved. This new model and the surface potential calculation give accurate values for the inversion charge in the useful range of MOS transistor operation. Some subtle differences between the inversion charges calculated from the two models were found. Both models give the same results for the inversion charge in weak inversion, $UCCM^+$ is better than the charge-sheet model in moderate inversion and the opposite is valid in strong inversion. Concerning the bulk charge modeling, no better option than the calculations based on the surface potential has been found.

REFERENCES

[1] M. Miura-Mattausch, U. Feldmann, A. Rahm, M. Bollu, and D. Savignac, "Unified complete MOSFET model for analysis of digital and analog circuits," *IEEE Trans. Computer-Aided Design*, vol. 15, pp. 1–7, January 1996.

[2] C. Galup-Montoro, M. C. Schneider, and A. I. A. Cunha, "A current-based MOSFET model for integrated circuit design," Chapter 2 of Low-Voltage/Low-Power Integrated Circuits and Systems, pp 7-55, edited by E. Sánchez-Sinencio and A. Andreou, IEEE Press, 1999.

[3] R. van Langevelde, A. J. Scholten, and D. B. M. Klaassen, "Physical Background of MOS Model 11**",** Nat. Lab. Unclassified Report 2003/00239. April 2003. (available on line at http://www.semiconductors.philips.com/Philips_Models/)

[4] G. Gildenblat, H. Wang, T.-L. Chen, X. Gu, and X. Cai, "SP: An advanced surface-potential-based compact MOSFET model", *IEEE J. Solid-State Circuits*, vol. 39, no. 9, pp. 1394-1406, September 2004.

[5] C. Enz, F. Krummenacher and E. A. Vittoz, "An analytical MOS transistor model valid in all regions of operation and dedicated to low-voltage and low-current applications," *Analog Integrated Circuits and Signal Processing Journal*, vol. 8, pp. 83-114, July 1995.

[6] W. Liu *et al.*. (1999) BSIM3v3 Manual. Dept. Elect. Eng. Comp. Sci., Univ. California,Berkeley. [Online]. Available: http://wwwdevice.eecs.berkeley.edu/~bsim3/get.html

[7] M. A. Maher and C. A. Mead, "A physical charge-controlled model for MOS transistors," in *Advanced Research in VLSI*, P. Losleben (ed.), MIT Press, Cambridge, MA, 1987.

[8] Y. Byun, K. Lee and M. Shur, "Unified charge control model and subthreshold current in heterostructure field effect transistors," *IEEE Electron Device Letters*, vol. 11, no. 1, pp. 50-53, January 1990.

[9] J.-M. Sallese, M. Bucher, F. Krummenacher, and P. Fazan, "Inversion charge linearization in MOSFET modeling and rigorous derivation of the EKV compact model", *Solid-State Electronics* vol. 47, pp. 677–683, 2003.

[10] J. He, X. Xi, M. Chan, A. Niknejad, and C. Hu, "An advanced surface potential-plus MOSFET model," p. 262 in *Tech. Proc. 2003 Nanotechnology Conf.*

[11] Y. Tsividis, *Operation and modeling of the MOS transistor*, 2nd edition, McGraw-Hill, New York, 1999.

[12] H. C. Pao and C. T. Sah, "Effects of Diffusion Current on Characteristics of Metal-Oxide (Insulator)-Semiconductor Transistors," *Solid-State Electron.*, Vol. 9, pp. 927-937, 1966.

[13] J. R Brews, "A charge sheet model for the MOSFET," *Solid-State Electronics*, vol.21, pp.345-355, 1978.

[14] A. I. A. Cunha, M. C. Schneider, and C. Galup-Montoro, "An explicit physical model for the long-channel MOS transistor including small-signal parameters," *Solid-State Electronics*, vol. 38, no 11, pp. 1945-1952, November 1995.

[15] A. I. A. Cunha, M. C. Schneider, and C. Galup-Montoro, "Derivation of the unified charge control model and parameter extraction procedure," *Solid-State Electronics*, vol. 43, no 3, pp. 481-485, March 1999.

[16] A. I. A. Cunha, M. C. Schneider, and C. Galup-Montoro, "An MOS transistor model for analog circuit design," *IEEE J. Solid-State Circuits*, vol. 33, no 10, pp. 1510-1519, October 1998.

[17] BSIM5 presentation by Professor A. Niknejad [Online]. Available http://www.eigroup.org/cmc/minutes/default.htm

[18] A. T. Behr, M. C. Schneider, S. N. Filho, and C. Galup-Montoro, Harmonic distortion caused by capacitors implemented with MOSFET gates", *IEEE Journal of Solid-State Circuits*, vol. 27, no. 10, pp. 1470-1475, October 1992.

[19] R. Rios, S. Mudanai, W.-K. Shih, and P. Packan, "An Efficient Surface Potential Solution Algorithm for Compact MOSFET Models," pp 755-758. *IEDM 2004 Tech. Dig*.

[20] N. Arora, *"MOSFET Models for VLSI Circuit Simulation Theory and Practice*," Springer-Verlag, Wien, 1993.

[21] F. V. de Wiele, "A Long-channel MOSFET model", *Solid-State Electronics*, vol. 22, no 12, pp. 991-997, December 1979.